Functionalized 4,4'-bipyridines: synthesis and 2D-organization on HOPG

Jimmy Richard, Jean Joseph, Can Wang, Artur Ciesielski, Jean Weiss, Paolo Samorì, Victor Mamane, Jennifer A Wytko

Functionalized 4,4'-bipyridines: synthesis and 2D-organization on HOPG

Jimmy Richard,[†,§,&] Jean Joseph,[†,&] Can Wang,[‡] Artur Ciesielski,[‡] Jean Weiss,[†] Paolo Samorì,[‡,*] Victor Mamane,[†,*] and Jennifer A. Wytko[†,*]

[†] Institut de Chimie de Strasbourg, UMR 7177, CNRS-Université de Strasbourg, 1 rue Blaise Pascal, 67000 Strasbourg, France.

[‡] Université de Strasbourg and CNRS, ISIS, 8 allée Gaspard Monge, 67000 Strasbourg, France

KEYWORDS. 4,4'-bipyridine, nitrogen heterocycles, cross-coupling, STM, 2D nanopatterns

ABSTRACT: Commercial 4,4'-bipyridine is a popular scaffold which is primarily employed as a linker in 3D self-assembled architectures such as metallo-organic frameworks or as connector in 2D networks. The introduction of alkyl substituents on the bipyridine skeleton is instrumental when 4,4'-bipyridines are used as linkers to form 2D self-assembled patterns on surfaces. Here, various synthetic strategies to access 4,4'-bipyridines functionalized at various positions are described. These easily scalable reactions have been used to introduce a range of alkyl substituents at positions 2 and 2', or 3 and 3' and at positions 2,2' and 6,6' in the case of tetra-functionalization. Scanning tunneling microscopy studies of molecular monolayers physisorbed at the graphite-solution interface revealed different supramolecular patterns whose motifs are primarily dictated by the nature and position of the alkyl chains.

INTRODUCTION

In the bipyridine family, the 2,2'-bipyridine chelate represents the most popular scaffold for the formation of discrete metal complexes. As a result, a large variety of functional groups have been introduced on 2,2'-bipyridine over the last decades.[1] On the contrary, relatively few synthetic strategies leading to functionalized 4,4'-bipyridine (4,4'-bipy) have been developed due to the quasi exclusive use of this ligand as a linker between metals or metal complexes,[2] for example in luminescent coordination polymers[3] and macrocyclic supramolecular species.[4] However, when used in combination with metal complexes with a restricted geometry, 4,4'-bipy can be employed as a building block for the generation of both polymeric and discrete supramolecular polygonal structures with controlled geometries such as squares or rectangles.[5] The absence of chelating abilities makes 4,4'-bipy binding less entropically-controlled than with 2,2'-bipyridine. Therefore, in most cases, in the solid state 4,4'-bipy assembles with metals into supramolecular polymers or organized frameworks. In the latter, the linear, rigid structure of 4,4'-bipy makes it possible to control the structure and morphology of metal-organic-framework assembling processes,[6] yielding by design distinct properties useful for speciation,[7] luminescence[8] or molecular electronics.[9]

As a consequence of its geometric features, 4,4'-bipy is a versatile building block for the generation of supramolecular 2D networks which could self-assemble at the solid-liquid interface. Whereas shape persistent discrete self-assembled species characterized in solution have been deposited and observed on surfaces,[10] the most common use of 4,4'-bipy in surface self-assembly is as a mediator to control the deposition of carboxylic acids bearing long alkyl chains[11] or of building blocks functionalized with amides.[12] For the formation of self-assembled 2D networks on highly oriented pyrolytic graphite (HOPG), 4,4'-bipys are used as the bare ligand associated with other building blocks, (e.g. polycarboxylic acids) bearing alkyl chains. In the case of metallic surfaces, unsubstituted analogues have led, for example, to organized assemblies via coordination of surface adatoms on Cu(100).[13]

To increase the scope of 4,4'-bipy-based structures that self-organize on surfaces, in this paper, ether or alkyl chains are introduced at various positions of the 4,4'-bipy. Some synthetic approaches to introduce these substituents at two or four carbon atoms of the 4,4'-bipy skeleton are described. The methods described below can be extended to enable the introduction of various functional groups on the 4,4'-bipy.

Two main strategies have been pursued to functionalize 4,4'-bipy, as depicted in Figure 1. In the first strategy, the preformed 4,4'-bipy skeleton is directly functionalized but substitution is only possible at positions *ortho* with respect to the heteroatoms. The Chichibabin reaction[14] is perhaps the most useful reaction because the resulting amine substituents are easily converted to other functional groups. Both 2,2'-diamino- and 2,2',6,6' tetraamino-4,4'-bipyridines have been obtained by means of this method.[15] The only other examples of the addition of four substituents to

4,4'-bipy are metal-mediated (Fe(II)[16] or Ag(I)[17]) radical additions of four acetyl substituents, although yields are low. Similar radical reactions have led to mono-substituted 2-methyl or 2-ethyl-4,4'-bipyridine.[18] Two functional groups can be efficiently added by first activating the 2,2' positions of 4,4'-bipy. *N*-oxides have proven to be useful intermediates to introduce chloro[19] or nitrile groups.[20] In addition, fluoride activation using acetyl hypofluorite[21] leads to addition of two acetoxy groups to 4,4'-bipy in excellent yield. A final method is a classical nucleophilic addition of organolithium reagents followed by oxidation of the resulting dihydro addition product.[22] Drawbacks of this method include low yields and mixtures of mono, di- and trisubstituted 4,4'-bipys.

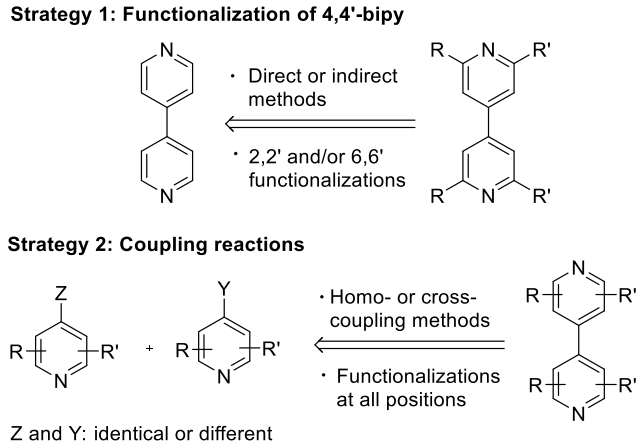

Figure 1. Two strategies to functionalize 4,4'-bipyridine.

The second strategy involves the homocoupling or cross-coupling of prefunctionalized pyridines to generate the 4,4'-bipy with nearly any desired substitution pattern. The homocoupling methods require alkali/alkali earth reagents (Na,[23] Mg/Li,[24] LDA[25]), transition metals ($NiCl_2(PPh_3)_2$/Zn,[26] $Pd(OAc)_2$/In[27]), or both (LDA/$CuCl_2$,[28] RMgBr/$FeCl_3$[29]), and thus implies the chemical inertness of the functional groups present on the pyridine moieties. The moderate yields of many of these coupling reactions do not hamper this strategy due to the availability and the reasonable cost of some pyridine starting materials. However, in contrast to the wide variety of homocoupling methods, cross-coupling methods leading to 4,4'-bipys are limited and are either metal-catalyzed[30] or mediated by phosphorus.[31]

As in any synthesis, the substituents of the bipyridines obtained by either approach can be subjected to further modification. Despite the variety of functional groups that can be obtained, there are few examples of 4,4'-bipys bearing ether substituents or alkyl chains other than methyls or ethyls,[32] which might promote the physisorption of these molecules on surfaces.

RESULTS AND DISCUSSION

2,2'-Substituents. Our first target molecule was a 4,4'-bipy with two long chains at the 2,2' positions. The most direct route to such molecules was via the nucleophilic addition of alkyllithium reagents. Initial attempts to optimize reaction conditions using *n*-BuLi afforded a mixture of mono-, di- and tri-butyl substituted 4,4'-bipy, all with low yields, as well as unreacted 4,4'-bipy. The nucleophilic addition of a Grignard reagent with a long alkyl chain ($ClMgC_{18}H_{37}$) also failed and these methods were not pursued any further. In a less direct synthesis inspired by work of Fürstner,[33] a Kumada coupling reaction of 2,2'-dichloro-4,4'-bipyridine[19] (**1**) with $ClMgC_{18}H_{37}$ in the presence of 10 mol% $Fe(acac)_3$ gave the dialkyl product **2** in 34% yield (Scheme 1). In addition, 4,4'-bipy, resulting from dehalogenation, was recovered in 10% yield from a mixture containing other side products.

Scheme 1. Iron-catalyzed coupling reaction to introduce two long alkyl chains.

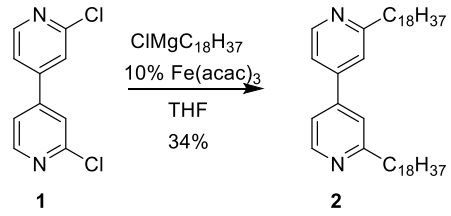

Scheme 2. Use of a Wittig reaction to introduce four alkyl chains.

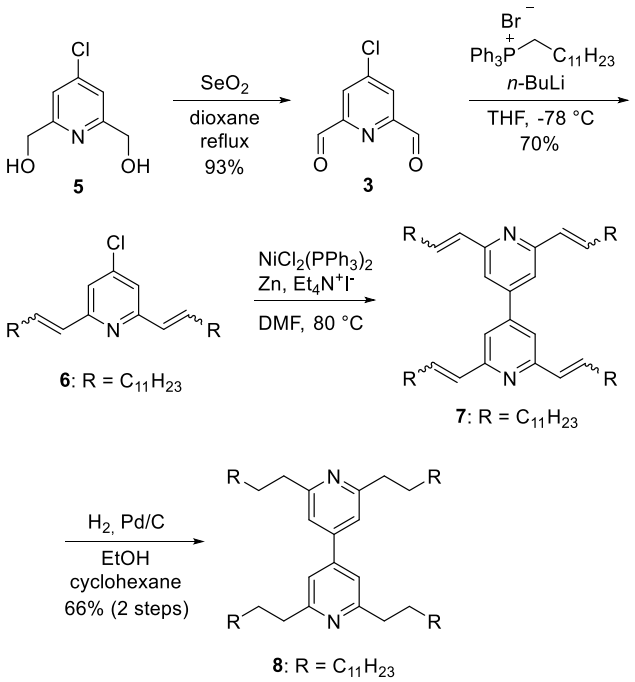

An alternative path to di- or tetra-alkyl derivatives makes use of aldehydes **3** (Scheme 2) and **4** (Scheme 3) that can serve for the efficient formation of Wittig adducts. The pyridine dialdehyde **3** was prepared in 93% yield by oxidation of the hydroxymethyl groups of **5** with selenium dioxide.[34] The yield of this oxidation was considerably lower with pyridinium dichromate (41% yield). A subsequent Wittig reaction with a dodecyl phosphonium bromide salt[35] and *n*-BuLi as a base furnished **6** as a mixture of stereoisomers. Rather than separating this complex mixture of compounds with very close R_f values on silica gel, the salts were

simply removed by filtration on a Celite® plug and the mixture was used for the next step. Homocoupling of **6** in the presence of Ni(II)/Zn(0)[26] to generate bipyridine **7** and subsequent reduction of the alkenes with H_2 and Pd/C afforded the tetraalkyl-bipyridine **8** in 66% yield over two steps. Hydrogenation of **6** prior to the coupling reaction was a dead end due to reductive dehalogenation of the chloride function (H_2, Pd/C in EtOH) or lack of reaction (H_2, Pd/C in THF). Whereas the presence of four long alkyl chains of bipyridine **8** should provide strong surface-molecule interactions, we were not certain that only two alkyl chains would suffice. Consequently, a bis-gallyl derivative **9** (Scheme 3) with six octadecyloxy chains seemed more suitable for bis-functionalized derivatives. The synthesis of the required dialdehyde precursor **4** was previously reported as an eight-step procedure[36] starting from 2-methylpyridine. This dialdehyde can now be prepared in only five steps from the same inexpensive starting material as shown in Scheme 3. The oxidative coupling of 2-methyl pyridine,[37] which is the first step of this five-step synthesis, is not shown.

Scheme 3. Preparation of dialdehyde 4 and subsequent Wittig reaction.

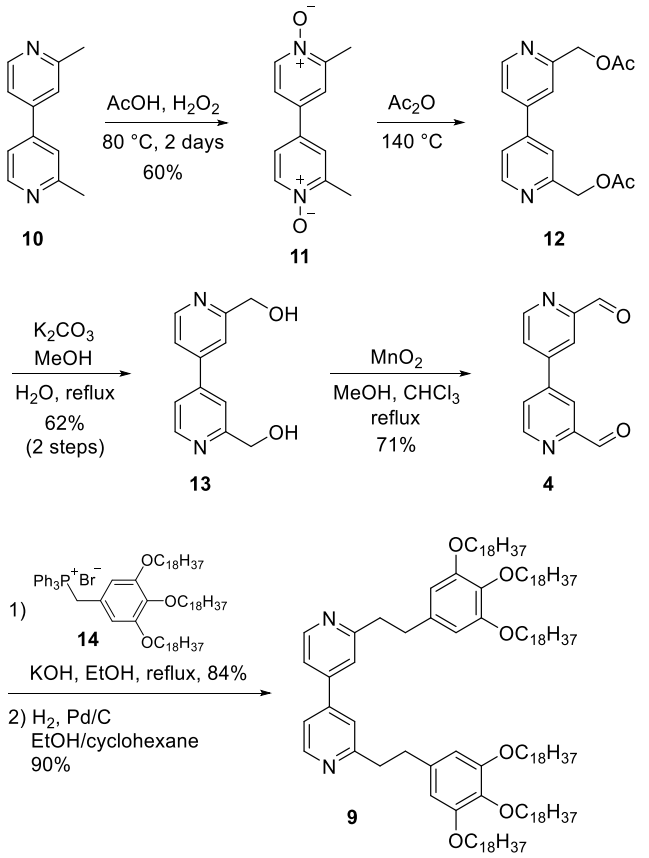

Treatment of 2,2'-dimethyl-4,4'-bipyridine (**10**)[37] with a mixture of $AcOH/H_2O_2$ at 80 °C for 2 days gave the corresponding *N*-oxide **11** in 60% yield. This *N*-oxide was converted to 2,2'-di(hydroxymethyl)-4,4'-bipyridine (**13**) in two steps by a Boekelheide rearrangement,[38] and in situ hydrolysis of the acetyl intermediate **12**. Oxidation of the alcohol functions of **13** with MnO_2[39] afforded dialdehyde **4** in 71% yield. Other oxidants were less efficient, with no reaction observed with SeO_2 and only 30% yield with pyridinium dichromate. In addition, attempts to directly oxidize the methyl substituents of 2,2'-dimethyl-4,4'-bipyridine (**10**) with SeO2 were unsuccessful. The two-step transformation of dialdehyde **4** to the desired bis-gallyl derivative **9** was achieved efficiently by a Wittig reaction with the gallyl-phosphonium bromide **14**[40] and subsequent reductive hydrogenation of the resulting mixture of alkene isomers (intermediate is not shown). The choice of base affected the yield of this Wittig reaction, where employing KOH gave much higher yields (84%) than did *n*-BuLi (44%).

3,3'-Substituents. To extend the family of alkyl-substituted bipyridines to compounds with less hindered nitrogen atoms, 3,3'-alkyl-substituted 4,4'-bipys were targeted. Because these positions are not activated on the 4,4'-bipy skeleton, the pyridine coupling strategy and post-transformation of substituents on the resulting bipyridine was adopted. The halogen substituents of 3,3'-dibromo-4,4'-bipyridine (**15**)[28] made this compound an ideal starting point. Based on the high yields of the Wittig reaction as a method to append alkyl substituents at positions *ortho* to the nitrogen atoms of the bipy, compound **16** bearing aldehydes at the 3,3'-positions was a desirable intermediate. Unfortunately, all attempts to convert the dibromide **15** to the dialdehyde **16** failed using halogen-lithium exchange in anhydrous THF or Et_2O, followed by quenching with dry DMF (Scheme 4). Numerous products were observed by TLC, but product **16** was never observed by ^1H NMR. When the reaction was carried out in dry toluene, an aldehyde peak was observed by ^1H NMR; unfortunately, dialdehyde **16** could not be isolated from the complex mixture of products. An alternative, two-step route *via* the dicyano derivative **17** to dialdehyde **16** was envisioned, as shown at the bottom of Scheme 4. Treatment of dibromide **15** with CuCN in refluxing *N*-methyl-2-pyrrolidine (NMP) yielded the dicyano intermediate **17** in 52% yield. However, reduction of **17** with DIBAL-H and subsequent acid and base treatment did not provide dialdehyde **16**.

Scheme 4. Attempts to prepare 3,3'-dialdehyde 16. Solvent = THF, ether or toluene.

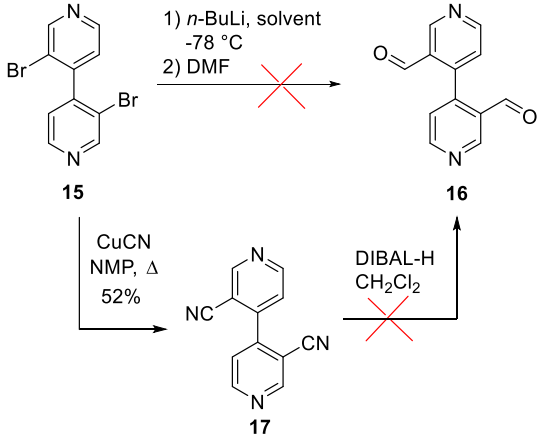

Sonogashira coupling was another possible method to functionalize dibromide **15**. When the commercially available dodec-1-yne was coupled with **15**, the tricyclic compound **18** was isolated in 64% yield instead of the desired coupling product **19** (shown in Scheme 6). This type of tricyclic product was previously observed with biphenyl derivative.[41] According to the proposed mechanism, the introduction of the first alkyne function occurs as expected at one of the two C-Br bonds to give intermediate **A**. However, after the oxidative addition of the second C-Br bond to Pd(0), the intramolecular cyclization occurs faster than the transmetalation/reductive elimination of the second alkyne. The resulting alkenylpalladium species **B** finally reacts with the second alkyne to furnish the observed cyclized product **18** (Scheme 5).

Scheme 5. Attempted Sonogashira reaction with 3,3'-dibromo-4,4' bipyridine 15.

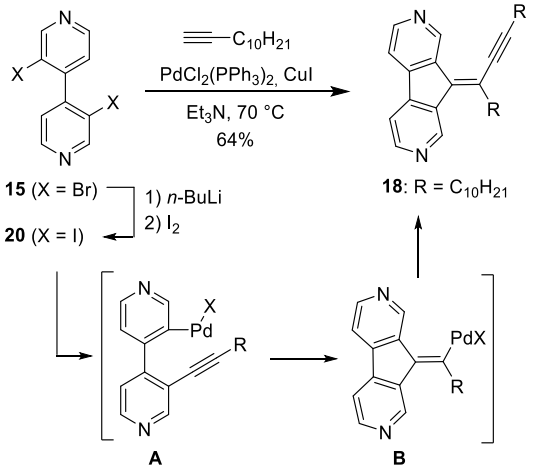

To prevent the formation of this compound, our first strategy was to accelerate the oxidative addition of Pd(0) by using 3,3'-diiodo-4,4'-bipyridine (**20**). The latter was prepared by lithium-halogen exchange starting from the dibromo-derivative **15** (Scheme 5). Once again, the coupling reaction afforded the cyclized product at 70 °C whereas no conversion was observed at room temperature. Our second strategy consisted in increasing the concentration of the alkynylmetal intermediate. The Negishi coupling was therefore selected because (sub)stoichiometric amounts of alkynylzinc species are used in contrast to the Sonogashira coupling where the alkynylcopper intermediate is formed only in catalytic amounts. Indeed, applying Negishi coupling conditions successfully afforded bipyridine **19** in a moderate 49% yield (Scheme 6). Trimethylsilyl-protected alkynes were also introduced via Negishi coupling to yield the bis-TMS derivative **21** in 49% yield. The yields of both Negishi coupling reactions are acceptable considering that two simultaneous reactions occur at hindered aryl bromides. Single-crystals of the bis-TMS derivative **21** were obtained by slow evaporation of the solvents (CH2Cl2/cyclohexane 2:1).

Scheme 6. Negishi coupling reaction with 3,3'-dibromo-4,4' bipyridine 15.

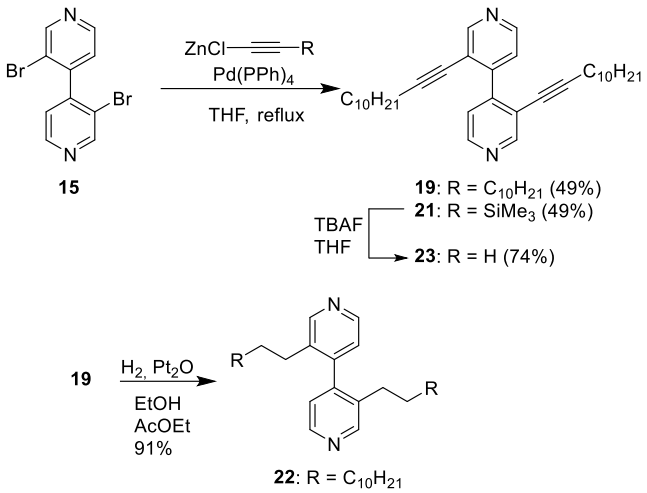

The X-ray structure of **21** depicted in Figure 2 shows a dihedral angle of 55.26° between the two pyridine planes. This angle is larger than that of the unsubstituted 4,4'-bipy structure (34.85°) measured at low temperature,[42] yet considerably smaller than the 81.8° observed in the structure of 3,3'-dimethyl-4,4'-bipyridine.[43] Thus, the triple bonds of compound **21** decrease the dihedral angle between the two aromatic rings of the bipyridine, and are expected to allow significant surface-molecule interactions in derivatives bearing longer alkyl chains. For the sake of comparison, the reduced alkane derivative **22** was also of interest for surface deposition. Thus, hydrogenation of **19** in the presence of PtO_2 in a mixture of EtOH/EtOAc gave **22** in high yield.

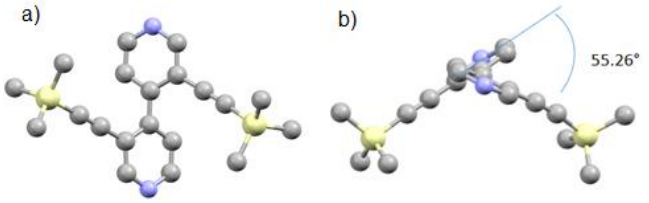

Figure 2. a) Top and b) side-views of the X-ray structure of **21**.

To extend the alkyne to substituents that would adhere to an HOPG surface, compound **24** bearing four ether chains was prepared by a Negishi coupling. Deprotection of the alkynes of **21** (Scheme 6) with TBAF afforded **23**. Treatment of this terminal alkyne with *n*-BuLi then $ZnCl_2$ furnished the organozinc intermediate **25** that was coupled with arylbromide **26** to give the bipyridine **24** in 62% yield (Scheme 7). It should be noted that no reaction occurred under Sonogashira coupling conditions between **23** and aryl bromide **26**.

Scheme 7. Addition of aromatic ethers by a Negishi Coupling.

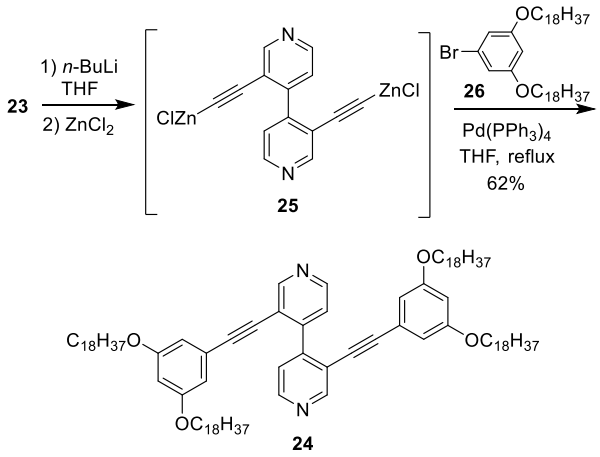

On-surface organization. Compounds **2**, **8**, **9**, **19**, **22** and **24** were expected to be good candidates for surface patterning, keeping in mind that 4,4'-bipys are often used as connectors in 1D/2D/3D self-assembled molecular architectures. To confirm the ability of 2,2' and 2,2',6,6' or 3,3' functionalized 4,4'-bipys to physisorb and organize on surfaces into ordered supramolecular structures, scanning tunneling microscopy (STM) imaging was employed at the interface between HOPG and a solution of the given molecule in 1-phenyloctane under ambient conditions. The samples were prepared by drop casting 4 µL of a 1 mM solution onto a freshly cleaved HOPG surface.

STM experiments revealed that 2,2'-substituted 4,4'-bipys (**2**, **8**, **9**) are more prone to self-assemble into ordered patterns than 3,3'-substituted bipys (**19**, **22**, **24**). As shown in Figure 3, compounds **2**, **8**, and **9** formed highly ordered 2D supramolecular assemblies stabilized via van der Waals interactions between the molecules and the underlying HOPG surface. As a result of the occurrence of resonant tunneling between the Fermi level of the HOPG and the frontier orbital of the adsorbate, the brighter areas in the STM images can be ascribed to the aromatic cores (i.e. 4,4'-bipys and phenylenes). Due to the planar conformation of the 4,4'-bipy cores, all three molecules packed in a face-on fashion onto the basal plane of the HOPG surface.

All unit cell parameters of compounds **2**, **8** and **9** are reported in Table 1. The differences in the packing motifs are mostly caused by the different nature and number of alkyl chains attached to the bipyridine cores, which results in larger unit cell area with increased number of alkyl substituents.

Table 1. Unit cell[a] parameters of self-assembled structures on HOPG surface based on the STM results.

Compound	a (nm)	b (nm)	γ (°)
2	1.0 ± 0.1	2.9 ± 0.1	85 ± 2
8	1.8 ± 0.1	2.2 ± 0.1	60 ± 2
9	2.7 ± 0.1	3.3 ± 0.1	66 ± 2
24	1.9 ± 0.1	3.1 ± 0.1	83 ± 2

[a] All unit cells contain one molecule.

In agreement with literature data for 2,2'-bipyridines,[44] the two C_{18} alkyl chains on compound **2** seem sufficient to ensure the physisorption on HOPG whereas four chains are needed when using shorter alkyl substituents (C_{13}). Intermolecular interactions favor a packing motif in which the shorter alkyl chains are not interdigitated but simply arranged in an anti-parallel fashion to maximize van der Waals contacts, in good agreement with previous reports on 2,2'-bipyridines bearing four octyl chains.[45] Bipyridine **9** shows a compact 2D arrangement due to both the number and the length of the alkoxy chains. All six alkoxy chains (OC_{18}) per molecule participated in the assembled structure to fill the bare area between the rows of aromatic cores (Figure 3e-f).

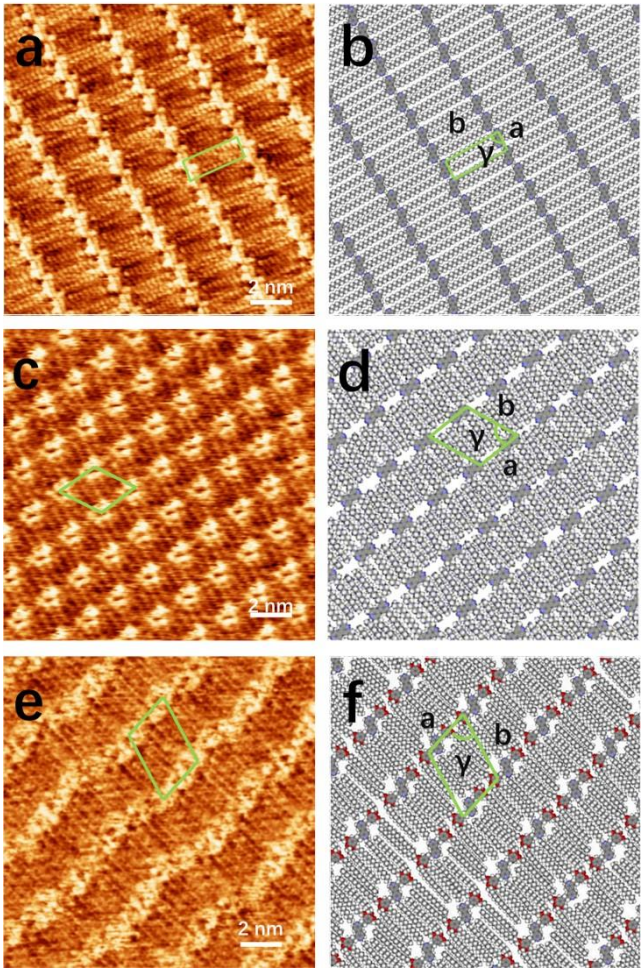

Figure 3. High-resolution STM height images recorded at the solution-graphite interface (a, c, e) and respective proposed packing motifs (b, d, f) for molecules **2**, **8** and **9**, respectively. Tunneling parameters: (a) tunneling voltage (V_t)= 500 mV and average tunneling current (I_t) = 30 nA; (c) V_t = 450 mV and I_t = 35 nA; (e) V_t = 530 mV and I_t = 40 nA.

The self-assembled structures of compounds **2** and **9** are mainly governed by van der Waals interactions between the alkyl chains. The differences in the arrangement are caused by the different number of carbon atoms in the alkoxy side chains. Compared to **2**, compound **9** contains four more carbon chains and a lager aromatic core structure. The two alkoxy chains at the para positions of the two

phenyls adopt their assembly on HOPG parallel to the direction of other chains (Figure S1), which leads to a lower regularity in the orientation of the aromatic cores.

The self-assembly behavior of 4,4'-bipy substituted at the 3,3' positions was expected to be significantly different due to the inherent dihedral angle imposed by the substituents. As a result of the steric hindrance of an sp^3 carbon, compound **22**, which bears two C_{12} saturated alkyl chains does not self-assemble at the liquid/HOPG interface into ordered supramolecular structures. Compound **19** also did not adsorb on the HOPG surface despite the presence of a less hindered sp hybridized substituent at the 3 and 3' positions of the 4,4'-bipy.

Compared to **19**, compound **24** has improved features including two large aromatic cores and four additional extended side chains that can enhance the interaction between molecules and substrate. Thus, **24** was subsequently investigated and was found to self-assemble into a highly ordered 2D structure at the 1-phenyloctane/HOPG interface; Figures 4a and 4b display the high-resolution STM image of **24** and the suggested model. The strong interaction between the long alkyl chains dominates the assembly. All four alkoxy chains (OC_{18}) per molecule are arranged in an anti-parallel fashion at a 75° angle with respect to the orientation of the tail of the aromatic core. The regular arrangement observed is consistent with the model proposed. According to the synthetic scheme leading to **24**, the regular spacing between the 4,4'-bipy moieties should be tuneable and is not limited to C_{18} substituents.

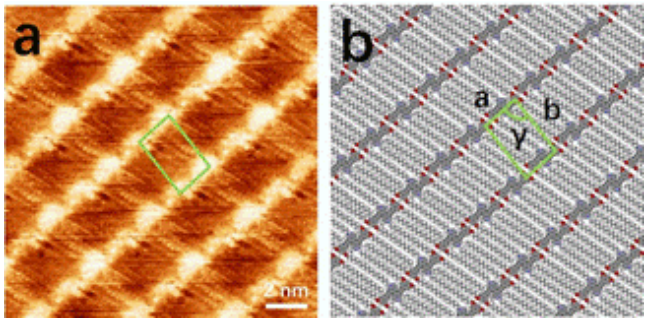

Figure 4. High-resolution STM height images of compound **24** self-assembled structure recorded at the solution-graphite interface (a) and respective proposed packing motif (b). Tunneling parameters: V_t = 500 mV and I_t = 50 nA.

CONCLUSION

Here we have demonstrated that 4,4'-bipy is a versatile scaffold that can self-assemble on the HOPG surface to adopt structural motifs that are governed by the substituents. Synthetic methods were developed first to functionalize 4,4'-bipy at the 2,2' and/or 6,6' or at the 3,3' positions, then to introduce substituents appropriate for physisorption on HOPG. The position and length of the substituents are the major factors determining the surface patterning. Independent on the number of alkyl/alkoxy chains of **2**, **8** and **9** with 2,2' and/or 6,6' substituents, all three compounds formed organized assemblies on HOPG. On the contrary, the steric hindrance imposed by the substituents at the 3,3' positions prevented molecules **19**, **22** and **24** from adopting a co-planar configuration of their pyridyl rings. Nevertheless, compound **24** with additional side chains and a lager aromatic core was capable of self-assembling on the HOPG surface. The broad synthetic versatility makes it possible to generate supramolecular architectures with notably different motifs. Moreover, the high solubility of theses functionalized 4,4'-bipys also paves the way for their use in developing solution-processable self-assembled coordination polymers based on 4,4'-bipys as connectors. These new perspectives are currently under investigation.

EXPERIMENTAL PROCEDURES

General methods: Compounds **1**,[19] **5**,[34] **10**,[37] **14**,[40] and **15**[28] were prepared according to literature procedures. Octadecylmagnesium chloride solution (0.5 M in THF) was purchased from Aldrich (394262). MnO_2 (activated ⩽90%) was purchased from Honeywell (63548). THF was distilled over Na/benzophenone and NEt_3 was dried and distilled over NaOH. $ZnCl_2$ was dried by melting under high vacuum with a heat gun. The heating was stopped when the compound started to bubble, and a white coating appeared in the flask. After cooling to rt, the flask was filled with argon and the crystalline reagent was dissolved in the desired amount of solvent before addition to the organolithium. Unless indicated otherwise, DrySyn heating blocks were used to heat reactions.

Column chromatography was performed with silica gel from Merck (Kieselgel 60; 63-200 µm or 40-63 µm). ^1H NMR spectra were recorded on Bruker Advance 300 (300 MHz), 400 (400 MHz) or 500 (500 MHz) spectrometers. Chemical shifts were determined by taking the solvent as a reference. Mass spectrometry (MS and HRMS) experiments were performed on a Bruker Daltonics microTOF spectrometer (Bruker Daltonik GmgH, Bremen, Germany) by the Service de Spectrométrie de Masse de la Fédération de Chimie "Le Bel" (FR 2010).

STM investigations were performed by using a commercial multimode Nanoscope III scanning tunneling microscope with mechanically cut Pt/Ir (80:20) tips at ambient temperature. The images shown were recorded in constant-current mode if not indicated otherwise. For measurements at the liquid/substrate interface, a 4 µL drop of a 1 mM solution is applied onto a freshly cleaved surface of highly orientated pyrolytic graphite (HOPG). Different tips and samples were used to check for reproducibility and to ensure that there were no image artifacts caused by the tips or samples. Measurements obtained from STM images are corrected against the substrate lattice parameters obtained from HOPG images. Flattening of the images was carried out to compensate for the tilting of the substrate and scan line artifacts, and a low-pass-filtered transform was employed to remove scanning noise in the STM images.

Crystals suitable for X-ray analysis (see ESI) of compound **21** were obtained by slow evaporation of the solvents (CH_2Cl_2/cyclohexane, 2:1). Deposition Number 2042158 contains the supplementary crystallographic data for this paper. These data are provided free of charge by the joint

Cambridge Crystallographic Data Centre and Fachinformationszentrum Karlsruhe Access Structures service www.ccdc.cam.ac.uk/structures.

2,2'-Dioctadecyl-4,4'-bipyridine (**2**). An octadecyl-magnesium chloride solution (20 mL, 20 mmol, 0.5 mol/L) was added to 2,2'-dichloro-4,4'-bipyridine[19] **1** (0.5 g, 2.22 mmol) and tris(acetylacetonato)iron(III) (78 mg, 0.22 mmol) in degassed THF (60 mL) at 0 °C. The orange mixture becomes immediately dark purple. The mixture was stirred under argon at r.t. for 1 h. Water (50 mL) and diethyl ether (50 mL) were added. The aqueous layer was extracted twice with diethyl ether and the combined organic phases were washed with water. The organic phase was dried over sodium sulfate, filtered and concentrated. The residue was purified by column chromatography (SiO_2, CH_2Cl_2) to afford compound **2** as a white-beige solid (500 mg, 0.756 mmol, 34%). mp 61 °C; ^{1}H NMR ($CDCl_3$, 500 MHz) δ 8.63 (d, *J* = 5.0 Hz, 2H), 7.36 (s, 2H), 7.33 (dd, *J* = 5.0, 1.9 Hz, 2H), 2.86 (t, *J* = 7.9 Hz, 4H), 1.77 (quint, *J* = 7.9 Hz, 4H), 1.41-1.32 (m, 8H), 1.32-1.20 (m, 52H), 0.87 (t, *J* = 6.9 Hz, 6H); ^{13}C{^{1}H} NMR ($CDCl_3$, 126 MHz) δ 163.7, 150.1, 146.4, 120.6, 119.0, 38.7, 32.1, 30.2, 29.9, 29.82, 29.81, 29.72, 29.66, 29.62, 29.5, 22.6, 14.3; MS (ESI) *m/z* calcd for $C_{46}H_{81}N_2$: 661.64 $[M+H]^+$; found 661.64; Anal. Calcd for $C_{46}H_{80}N_2$: C, 83.57; H, 12.20; N, 4.24. Found: C, 83.16; H, 12.31; N, 4.19.

4-Chloropyridine-2,6-dicarbaldehyde (**3**). Selenium oxide powder (3.09 g, 27.8 mmol) was added to a solution of (4-chloropyridine-2,6-diyl)dimethanol[34] **5** (2.30 g, 13.2 mmol) in 1,4-dioxane (50 mL). The mixture was stirred under argon at reflux for 5 h. After cooling to r.t., the black solid was filtered and the orange filtrate was concentrated. The crude solid was purified by column chromatography (SiO_2, $CHCl_3$) to afford compound **3** as a beige solid (2.09 g, 12.33 mmol, 93%). The product was characterized by comparison with literature data.[46]

4-Chloro-2,6-di(tridec-1-en-1-yl)pyridine (**6**). *n*-Butyllithium (12.1 mL of a 1.6 M solution in hexane, 19.4 mmol) was added dropwise to a solution of triphenyl(tridecyl)phosphonium bromide (9.90 g, 19.3 mmol) in THF (100 mL) at -78 °C under argon. The orange mixture was stirred under argon at -78 °C for 30 min. Then a solution of 4-chloropyridine-2,6-dicarbaldehyde **3** (1.49 g, 8.81 mmol) in THF (20 mL) was added to the mixture. The mixture was stirred under argon at -78 °C for 1 h then at r.t. for 10 h. The mixture was concentrated and the residue was purified by column chromatography (SiO_2, CH_2Cl_2) to afford compound **6** as a white solid (2.92 g, 6.17 mmol, 70%). The product was used for the next step after characterization by ^{1}H NMR only. ^{1}H NMR ($CDCl_3$, 400 MHz) δ 7.22-7.85 (m, 2H), 6.98-7.06 (m, 1H), 6.54-6.65 (m, 2H), 6.10-6.16 (m, 1H), 2.82-2.86 (m, 2H), 2.46-2.48 (m, 2H), 1.49-1.73 (m, 36H), 1.10 (t, *J* = 6.8 Hz, 6H).

2,2',6,6'-Tetratridecyl-4,4'-bipyridine (**8**). Zinc powder (0.59 g, 9.3 mmol) was added to a solution of dichlorobis(triphenylphosphine)-nickel(II) (6.07 g, 9.3 mmol) in DMF (100 mL). After 2 h of stirring, the green solution turned red. Then tetraethylammonium iodide (2.39 g, 9.3 mmol) and 4-chloro-2,6-di(tridec-1-en-1-yl)pyridine **6** (4.00 g, 8.44 mmol) was added to the mixture. The mixture was stirred under argon at 80 °C (oil bath) for 18 h. After cooling to r.t., water (100 mL) and dichloromethane (100 mL) were added. The black solid was removed by a filtration through a small pad of Celite. The aqueous layer was extracted twice with dichloromethane and the combined organic phases were washed with water. The organic phase was dried over sodium sulfate, filtered and concentrated. The resulting oil was filtered over a column of SiO2 (CH_2Cl_2/cyclohexane, 1/1) to give **7** (3.19 g, 3.64 mmol) as a mixture of diastereoisomers. This mixture was dissolved in a mixture of cyclohexane/ethanol (120 mL/80 mL). Degassed palladium on carbon (10% wt, 0.72 g, 0.68 mmol) was added to the solution. The mixture was stirred under hydrogen (in a balloon) at r.t. for 3 days. The palladium was removed by filtration through a small pad of Celite. The mixture was concentrated and the beige solid was recrystallized from diethyl ether to afford compound **8** as a white solid (2.11 g, 2.38 mmol, 66%). mp 62 °C; ^{1}H NMR ($CDCl_3$, 500 MHz) δ 7.15 (s, 4H), 2.82 (t, *J* = 8.0 Hz, 8H), 1.74 (q, *J* = 8.0 Hz, 8H), 1.25-1.37 (m, 80H), 0.87 (t, *J* = 7.0 Hz, 12H); ^{13}C{^{1}H} NMR ($CDCl_3$, 126 MHz) δ 163.0, 147.1, 117.8, 38.9, 32.1, 30.5, 29.85, 29.83, 29.82, 29.81, 29.8, 29.7, 29.69, 29.5, 22.8, 14.3; MS (ESI) *m/z* calcd for $C_{62}H_{113}N_2$: 885.89 $[M+H]^+$; found 885.89; Anal. Calcd for $C_{62}H_{112}N_2$: C, 84.06; H, 12.75; N, 3.16. Found: C, 84.08; H, 12.44; N, 3.16.

2,2'-Dimethyl-[4,4'-bipyridine] 1,1'-dioxide (11). A mixture of 2,2'-dimethyl-4,4'-bipyridine[37] **10** (570 mg, 3.09 mmol), acetic acid (20 mL, 0.35 mol) and hydrogen peroxide (30% in water, 10 mL, 0.1 mol) was stirred at 90 °C for two days. After cooling to r.t., the solvents were evaporated. The residue was dissolved in $CHCl_3$ (50 mL) then a saturated solution of NaCl was added (50 mL). The aqueous layer was extracted twice with $CHCl_3$ and the combined organic phases were washed with water. The organic phase was dried over sodium sulfate, filtered and concentrated. The residue was purified by column chromatography (SiO_2, CH_2Cl_2/MeOH, 10/1) to afford compound **11** as a white-beige solid (401 mg, 1.85 mmol, 60%). mp dec. > 180 °C; ^{1}H NMR ($CDCl_3$, 400 MHz) δ 8.29 (d, *J* = 6.7 Hz, 2H), 7.48 (d, *J* = 2.9 Hz, 2H), 7.36 (dd, *J* = 2.9, 6.7 Hz, 2H), 2.57 (s, 6H); ^{13}C{^{1}H} NMR ($CDCl_3$, 126 MHz) δ 149.7, 139.9, 133.1, 123.5, 120.7, 18.2; MS (ESI) *m/z* calcd for $C_{12}H_{13}N_2O_2$: 217.10 $[M+H]^+$; found 217.10. Anal. Calcd for $C_{12}H_{12}N_2O_2$: C, 66.65; H, 5.59; N, 12.96. Found: C, 66.55; H, 5.67; N, 12.78.

[4,4'-Bipyridine]-2,2'-diyldimethanol (**13**). A mixture of compound **11** (200 mg, 0.92 mmol) and acetic anhydride (20 mL, 0.21 mol) was heated under reflux under argon overnight. Then the solvent was evaporated. A mixture of the residue (intermediate **12**: ^{1}H NMR ($CDCl_3$, 500 MHz) δ 8.73 (d, J = 5.1 Hz, 2H), 7.57 (s, 2H), 7.47 (dd, J = 5.1, 1.9 Hz, 2H), 5.31 (s, 4H), 2.19 (s, 6H)), K_2CO_3 (500 mg, 3.6 mmol), MeOH (10 mL) and H_2O (2 mL) were stirred at r.t. overnight. $CHCl_3$ (50 mL) and a NaCl saturated solution were added (50 mL). The aqueous layer was extracted twice with $CHCl_3$ and the combined organic phases were washed with water. The organic phase was dried over sodium sulfate, filtered and concentrated. The residue was purified by column chromatography (SiO_2, CH_2Cl_2/MeOH 10/1) to afford compound **13** as a white solid (121 mg, 0.56 mmol, 62%) that

was used without further purification due to its limited solubility. mp >300 °C; ^{1}H NMR ($CDCl_3$, 400 MHz) δ 8.68 (d, *J* = 5.4 Hz, 2H), 7.53 (s, 2H), 7.45 (d, *J* = 5.4 Hz, 2H), 4.86 (s, 4H); MS (ESI) *m/z* calcd for $C_{12}H_{13}N_2O_2$: 217.10 $[M+H]^+$; found 217.10; Anal. Calcd for $C_{12}H_{12}N_2O_2$: C, 66.65; H, 5.59; N, 12.96. Found: C, 66.75; H, 5.70; N, 12.71.

[4,4'-Bipyridine]-2,2'-dicarbaldehyde (**4**). A mixture of compound **13** (105 mg, 0.54 mmol) and MnO_2 (201 mg, 2.31 mmol) in $CHCl_3$ (10 mL) was heated under refluxed under argon for 2 h. The mixture was filtered and the filtrate was concentrated. The residue was purified by column chromatography (SiO_2, CH_2Cl_2/MeOH, 10/1) to afford compound **4** as a white-yellow solid (81 mg, 0.381 mmol, 71%). The product was characterized by comparison with literature data.[36]

Compound 9. A mixture of **4** (42 mg, 0.20 mmol), compound **14**[40] (540 mg, 0.44 mmol) and KOH (34 mg, 0.6 mmol) in EtOH (40 mL) was refluxed under argon overnight. Then the solvent was evaporated. The residue was purified by column chromatography (SiO_2, CH_2Cl_2) to afford the alkene as a yellow solid (355 mg, 0.165 mmol, 84%). The product was used without further purification for the next step. A mixture of the alkene (200 mg, 0.101 mmol), palladium on carbon (10% wt, 11 mg, 0.01 mmol) in cyclohexane/EtOH (1/1 v/v, 20 mL) was stirred under hydrogen in a balloon at r.t. for 3 days. The palladium was removed by filtration over a small pad of Celite. The mixture was concentrated and the residue was purified by column chromatography (SiO_2, CH_2Cl_2) to afford compound **9** as a beige solid (185 mg, 0.090 mmol, 90%). mp 55 °C; ^{1}H NMR ($CDCl_3$, 500 MHz) δ 8.63 (d, J = 5.2 Hz, 2H), 7.34 (s, 2H), 7.27 (s, 2H), 6.38 (s, 4H), 3.95 – 3.81 (m, 12H), 3.18 – 2.95 (m, 8H), 1.74 (quint, J = 6.6 Hz, 8H), 1.67 (quint, J = 6.6 Hz, 4H), 1.47 – 1.39 (m, 12H), 1.34 – 1.26 (m, 168H), 0.87 (t, J = 6.9 Hz, 18H); ^{13}C{^{1}H} NMR ($CDCl_3$, 126 MHz) δ 161.3, 152.0, 149.1, 145.2, 135.5, 119.9, 118.0, 105.9, 72.8, 68.1, 39.7, 35.5, 30.9, 29.4, 28.8, 28.74, 28.69, 28.5, 28.4, 25.1, 21.7, 13.1; HRMS (ESI) *m/z* calcd for $C_{134}H_{241}N_2O_6$: 1974.8609 $[M+H]^+$; found 1974.8583.

[4,4'-Bipyridine]-3,3'-dicarbonitrile (**17**). A mixture of 3,3'-dibromo-4,4'-bipyridine[28] **15** (436 mg, 1.39 mmol) and CuCN (310 mg, 3.47 mmol) in NMP (5 mL) was heated at 200 °C overnight. After cooling to rt, a saturated aqueous solution of EDTA in 20% ammonia was added (150 mL). The resulting green solution was filtered and the residue was washed abundantly with water (800 mL). The filtrate was concentrated to 200 mL and extracted with ethyl acetate (3 x 50 mL). The organic phases were combined, dried over Na_2SO_4 and evaporated. The remaining NMP was removed under vacuum at 75 °C for 2 h. The residue was purified by column chromatography (SiO_2, CH_2Cl_2/AcOEt 3:1) to afford compound **17** (149 mg, 0.72 mmol, 52%) as a white solid. mp 180 °C; ^{1}H NMR ($CDCl_3$, 500 MHz) δ 9.10 (s, 2H), 9.00 (d, *J* = 5.2 Hz, 2H), 7.57 (d, *J* = 5.2 Hz, 2H); ^{13}C{^{1}H} NMR ($CDCl_3$, 126 MHz) δ 154.1, 153.7, 146.0, 123.7, 115.0, 109.0; HRMS (ESI) *m/z* calcd for $C_{12}H_7N_4$: 207.0665 $[M+H]^+$; found 207.0662.

9-(Tricos-12-yn-11-ylidene)-9H-cyclopenta[1,2-c:4,3-c']dipyridine (18). To a mixture of 3,3'-dibromo-4,4'-bipyridine[28] **15** (462 mg, 1.47 mmol), $PdCl_2(PPh_3)_2$ (103 mg, 0.15 mmol), copper(I) iodide (28 mg, 0.15 mmol) and 1-dodecyne (733 mg, 4.41 mmol) was added freshly distilled triethylamine (15 mL) under argon. The solution was stirred at 70 °C overnight. After evaporation of the solvents, the solid was taken in ethyl acetate and washed with water. The aqueous phase was extracted with ethyl acetate (3 x 10 mL). The combined organic phases were dried over Na_2SO_4, filtered and concentrated to dryness. The crude product was purified by column chromatography (SiO_2, cyclohexane/AcOEt, 2:1) to afford compound **18** (457 mg, 0.94 mmol, 64%) as a brown powder that contained traces of starting material **15** that were difficult to fully eliminate. ^{1}H NMR ($CDCl_3$, 500 MHz) δ 10.02 (s, 1H), 9.17 (s, 1H), 8.66 (m, 2H), 7.73 (dd, *J* = 18.9, 5.0 Hz, 2H), 2.98 (t, *J* = 7.9 Hz, 2H), 2.65 (t, *J* = 7.2 Hz, 2H), 1.84 (quint, *J* = 7.9 Hz, 2H), 1.74 (quint, *J* = 7.3 Hz, 2H), 1.55-1.47 (m, 4H), 1.43-1.37 (m, 4H), 1.36-1.27 (m, 20H), 0.89-0.85 (m, 6H); ^{13}C{^{1}H} NMR ($CDCl_3$, 126 MHz) δ 148.4, 148.1, 146.9, 146.6, 144.3, 143.4, 134.3, 133.9, 133.6, 131.8, 115.7, 115.0, 107.0, 83.6, 37.4, 32.0, 29.8, 29.8, 29.7, 29.7, 29.5, 29.5, 29.3, 28.9, 28.6, 22.8, 20.5, 14.3; MS (ESI) *m/z* calcd for $C_{34}H_{49}N_2$: 485.39 $[M+H]^+$; found 485.39. HRMS (ESI) *m/z* calcd for $C_{34}H_{49}N_2$: 485.3890 $[M+H]^+$; found 485.3889.

Compound 19. To a solution of 1-dodecyne (1.50 g, 9.0 mmol) in dry THF (30 mL) was added *n*-BuLi (6.0 mL of a 1.6 M in hexane, 9.6 mmol) at -78 °C under argon. The resulting solution was stirred for 30 min at this temperature and a solution of anhydrous $ZnCl_2$ (1.31 g, 9.6 mmol) in dry THF (7 mL) was added. After 30 min of stirring at -78 °C the solution was warmed to rt. This zinc derivative was then added via a double tipped needle to a solution of 3,3'-dibromo-4,4'-bipyridine[28] **15** (0.942 g, 3.0 mmol) and $Pd(PPh_3)_4$ (0.173 g, 0.15 mmol) in dry THF (15 mL) under argon. The mixture was refluxed overnight. After cooling to rt, the solution was quenched with 1 M HCl (5 mL) and then the THF was removed under vacuum. Water (15 mL) and CH_2Cl_2 (30 mL) were added and the aqueous phase was extracted with CH_2Cl_2 (3 x 15 mL). The combined organic phases were washed with H_2O (15 mL), dried over Na_2SO_4, filtered, and concentrated. The crude product was purified by column chromatography (SiO_2, cyclohexane/EtOAc, 4:1) to afford compound **19** (0.712 g, 1.47 mmol, 49%) as a beige solid. A sample of this compound was obtained as a white solid after a second column chromatography (SiO_2, cyclohexane, then cyclohexane/EtOAc, 4:1). mp 45 °C; ^{1}H NMR ($CDCl_3$, 500 MHz) δ 8.73 (s, 2H), 8.53 (d, *J* = 5.1 Hz, 2H), 7.32 (d, *J* = 5.1 Hz, 2H), 2.26 (t, *J* = 7.0 Hz, 4H), 1.41 (quint, *J* = 6.8 Hz, 4H), 1.26 (m, 28H), 0.88 (t, *J* = 6.8 Hz, 6H); ^{13}C{^{1}H} NMR ($CDCl_3$, 126 MHz) δ 153.4, 147.44, 147.36, 123.5, 120.0, 98.0, 76.2, 32.1, 29.8, 29.7, 29.5, 29.2, 28.9, 28.4, 22.8, 19.6, 14.3; HRMS (ESI) *m/z* calcd for $C_{34}H_{49}N_2$: 485.3890 $[M+H]^+$; found 485.3892; Anal. Calcd for $C_{34}H_{48}N_2$: C, 84.24; H, 9.98; N, 5.78. Found: C, 84.04; H, 9.84; N, 5.68.

3,3'-Diiodo-4,4'-bipyridine (**20**) To a solution of 3,3'-dibromo-4,4'-bipyridine[28] **15** (100 mg, 0.32 mmol) in dry THF (3 mL) was added *n*-BuLi (1.6 M, 0.5 mL, 0.80 mmol) at -78 °C under argon. The resulting orange solution was stirred 1 h then a solution of I_2 (203 mg, 0.80 mmol) in dry

THF (3 mL) was added. The solution was stirred 30 min then quenched with a saturated solution of NH_4Cl (10 mL). The mixture was warmed to rt and the aqueous phase extracted with ethyl acetate (3 x 20 mL). The organic layers were combined, washed with brine, dried over Na_2SO_4, filtered and concentrated. The crude was purified by column chromatography (SiO_2, cyclohexane/AcOEt 2:1) to afford compound **20** as a white solid (78 mg, 0.19 mmol, 60%). mp 148 °C; ^{1}H NMR ($CDCl_3$, 300 MHz) δ 9.08 (s, 2H), 8.65 (d, *J* = 4.8 Hz, 2 H), 7.13 (d, *J* = 4.8 Hz, 2H); ^{13}C{^{1}H} NMR ($CDCl_3$, 126 MHz) δ 157.9, 153.4, 149.3, 124.2, 97.0; HRMS (ESI) *m/z* calcd for $C_{10}H_7I_2N_2$: 408.8693 $[M+H]^+$; found 408.8693.

Compound 21. To a solution of trimethylsilylacetylene (1.33 g, 13.53 mmol) in dry THF (40 mL) was added *n*-BuLi (1.6 M in hexane, 8.90 mL, 14.07 mmol) at -78 °C under argon. The resulting solution was stirred 30 min at this temperature and a solution of anhydrous $ZnCl_2$ (1.92 g, 14.07 mmol) in dry THF (8 mL) was added. After 30 min of stirring at -78 °C the solution was warmed to rt. This zinc derivative was then slowly added via a double tipped needle to a solution of 3,3'-dibromo-4,4'-bipyridine[28] **15** (1.70 g, 5.41 mmol) and $Pd(PPh_3)_4$ (0.312 g, 0.27 mmol) in dry THF (25 mL) under argon. The mixture was refluxed overnight. After cooling to rt, the solution was quenched with 1 M HCl (5 mL) and the THF was evaporated. Water (15 mL) and CH_2Cl_2 (30 mL) were added and the aqueous phase was extracted with CH_2Cl_2 (3 x 15 mL). The organic phases were combined, washed with H_2O (15 mL), dried over Na_2SO_4, filtered, and concentrated. The crude product was purified by column chromatography (SiO_2, petroleum ether/ethyl acetate, 4:0.75) to afford compound **21** (0.92 g, 2.64 mmol, 49%) as a yellow solid. mp 99 °C; ^{1}H NMR ($CDCl_3$, 500 MHz) δ 8.79 (s, 2H), 8.57 (d, *J* = 5.1 Hz, 2H), 7.39 (d, *J* = 5.1 Hz, 2H), 0.10 (s, 18H); ^{13}C{^{1}H} NMR ($CDCl_3$, 126 MHz) δ 153.4, 148.3, 147.4, 123.5, 119.0, 102.6, 100.1, 0.4; HRMS (ESI) *m/z* calcd for $C_{20}H_{25}N_2Si_2$: 349.1551 $[M+H]^+$; found 349.1572.

Compound 22. To a suspension of PtO_2 (8 mg, 0.037 mmol) in a degassed mixture of 1:1 EtOH/EtOAc (1 mL) was added a solution of compound **19** (50 mg, 0.103 mmol) in the same solvents (1 mL) under argon. The solution was vigorously stirred under H_2 for 5 h. The mixture was filtered over a pad of Celite and rinsed with CH_2Cl_2. The solvents were evaporated to afford compound **22** (46 mg, 0.093 mmol, 91%) as a white solid, which was used without further purification. mp 51 °C; ^{1}H ($CDCl_3$, 500 MHz) δ 8.57 (s, 2H), 8.49 (d, *J* = 4.9 Hz, 2H), 7.00 (d, *J* = 4.9 Hz, 2H), 2.42 (td, *J* = 14.0, 7.8 Hz, 2H), 2.29 (td, *J* = 14.0, 7.8 Hz, 2H), 2.25 (q, *J* = 7.9 Hz, 2H), 1.40 (t, *J* = 7.2 Hz, 4H), 1.33–1.11 (m, 36H), 0.87 (t, *J* = 6.9 Hz, 6H); ^{13}C{^{1}H} NMR ($CDCl_3$, 126 MHz) δ 151.0, 147.1, 146.0, 135.3, 123.6, 32.1, 30.8, 30.6, 29.8, 29.8, 29.7, 29.6, 29.49, 29.46, 29.4, 22.8, 14.3; HRMS (ESI) *m/z* calcd for $C_{34}H_{57}N_2$: 493.4516 $[M+H]^+$; found 493.4516.

Compound 23. To a solution of compound **21** (846 mg, 2.43 mmol) in dry THF (10 mL) was added a solution of 1 M TBAF in THF (5.3 mL, 5.35 mmol) at rt under argon. The resulting black solution was stirred overnight, quenched with 1 M HCl (3 mL) and the solvent was evaporated. Water (15 mL) and CH_2Cl_2 (20 mL) were added to the solid and the aqueous phase was extracted with CH_2Cl_2 (3 x 15 mL). The organic phases were com-bined, washed with H_2O (15 mL), dried over Na_2SO_4 and concentrated. The residue was purified by column chromatography (SiO_2, cyclohexane/ethyl acetate/CH_2Cl_2, 2.5:2.5:1) to afford compound **23** (367 mg, 1.80 mmol, 74%) as a beige solid. The product was used for the next step without further purification. mp 191 °C; ^{1}H NMR ($CDCl_3$, 500 MHz) δ 8.86 (s, 2H), 8.65 (d, *J* = 5.1 Hz, 2H), 7.36 (d, *J* = 5.1 Hz, 2H), 3.16 (s, 2H); ^{13}C{^{1}H} NMR ($CDCl_3$, 126 MHz) δ 154.1, 149.0, 147.5, 123.5, 118.0, 84.4, 78.8; HRMS (ESI) *m/z* calcd for $C_{14}H_9N_2$: 205.0760 $[M+H]^+$; found 205.0757.

Compound 24. To a solution of 3,3'-diethynyl-4,4'-bipyridine **23** (100 mg, 0.49 mmol) in dry THF (2 mL) was added *n*-BuLi (1.6 M, 0.67 mL, 1.08 mmol) at -78 °C under argon. The mixture was stirred for 30 min at this temperature and a solution of anhydrous $ZnCl_2$ (167 mg, 1.22 mmol) in dry THF (2 mL) was added. After 30 min of stirring at -78 °C, the solution was warmed to rt. This zinc derivative was then slowly transferred via a double tipped needle to the solution of aryl bromide **26** (849 mg, 1.22 mmol) and $Pd(PPh_3)_4$ (28 mg, 0.02 mmol) in dry THF (6 mL) at rt under argon. The mixture was refluxed overnight, quenched with 1 M HCl (5 mL) and the THF was evaporated. Water (15 mL) and CH_2Cl_2 (30 mL) were added and the aqueous phase was extracted with CH_2Cl_2 (3 x 15 mL). The organic phases were combined, washed with H_2O (15 mL), dried over Na_2SO_4 and concentrated. The residue was purified by column chromatography (SiO_2, pentane/CH_2Cl_2 1:1; then pentane/AcOEt 4:1) to afford compound **24** (432 mg, 0.302 mmol, 62%) as a yellow solid. mp 75 °C; ^{1}H NMR ($CDCl_3$, 500 MHz) δ 8.91 (s, 2H), 8.65 (d, *J* = 5.1 Hz, 2H), 7.48 (d, *J* = 5.1 Hz, 2H), 6.43 (s, 2H), 6.42 (s, 4H), 3.86 (t, *J* = 6.5 Hz, 8H), 1.74 (quint, *J* = 6.5 Hz, 8H), 1.46–1.39 (m, 8H), 1.36–1.19 (m, 112H), 0.92–0.84 (m, 12H); ^{13}C{^{1}H} NMR ($CDCl_3$, 126 MHz) δ 160.2, 153.3, 148.3, 147.1, 123.8, 123.4, 119.3, 109.8, 103.3, 96.7, 84.3, 68.3, 32.1, 29.9, 29.85, 29.84, 29.82, 29.8, 29.7, 29.55, 29.52, 29.3, 26.2, 22.8, 14.3; HRMS (ESI) *m/z* calcd for $C_{98}H_{161}N_2O_4$: 1430.2451 $[M+H]^+$; found 1430.2443; Anal. Calcd for $C_{98}H_{160}N_2O_4$: C, 82.29; H, 11.28; N, 1.96. Found: C, 81.85; H, 11.19; N, 1.91.

Aryl bromide 26.[47] Argon was bubbled for 30 min in a suspension containing 5-bromoresorsinol (1.50 g, 7.9 mmol) and K_2CO_3 (3.29 g, 23.8 mmol) in DMF (45 mL). Then 1-bromooctadecane (6.61 g, 19.9 mmol) was added and the mixture was heated at 80 °C under argon for 16 h. After cooling to r.t. water was added (300 mL) and the suspension was extracted three times with dichloromethane (100 mL). The combined organic phases were washed with water twice, dried over sodium sulfate, filtered and concentrated. The crude material was purified by column chromatography (SiO_2, pentane). Then recrystallization from toluene and methanol afforded compound **26** as a white solid (3.97 g, 5.7 mmol, 72%). mp 59 °C; ^{1}H NMR ($CDCl_3$, 400 MHz) δ 6.64 (d, *J* = 2.2 Hz, 2H), 6.36 (t, *J* = 2.2 Hz, 1H), 3.90 (t, *J* = 6.6 Hz, 4H), 1.75 (tt, *J* = 7.4, 6.6 Hz, 4H),1.43 (tt, *J* = 7.4, 7.1 Hz, 4H),1.26 (m, 56H), 0.88 (t, *J* = 6.8 Hz, 6H); ^{13}C{^{1}H} NMR ($CDCl_3$, 126 MHz) δ 160.9, 122.9, 110.3, 100.7, 68.4, 32.1, 29.86, 29.85, 29.84, 29.82, 29.75, 29.71, 29.53,

29.50, 29.3, 26.1, 22.8, 14.3; HRMS (ESI) *m/z* calcd for $C_{42}H_{78}BrO_2$: 693.5180 $[M+H]^+$; found 693.5158.

ASSOCIATED CONTENT

Supporting Information. STM methods, X-Ray Crystallography Data, ^1H and ^{13}C NMR spectra, Mass spectra. This material is available free of charge via the Internet at http://pubs.acs.org.

AUTHOR INFORMATION

Corresponding Author

Victor Mamane – Institut de Chimie de Strasbourg, UMR 7177 CNRS-Université de Strasbourg, 4 rue Blaise Pascal, 67008 Strasbourg, France, vmamane@unistra.fr
Jennifer A. Wytko – Institut de Chimie de Strasbourg, UMR 7177 CNRS-Université de Strasbourg, 4 rue Blaise Pascal, 67008 Strasbourg, France, jwytko@unistra.fr
Paolo Samorì - ISIS, UMR 7006 CNRS-Université de Strasbourg, 8 allée Gaspard Monge, BP 70028, 67083 Strasbourg, France, samori@unistra.fr

Authors

Jimmy Richard – Institut de Chimie de Strasbourg, UMR 7177 CNRS-Université de Strasbourg, 4 rue Blaise Pascal, 67008 Strasbourg, France
Jean Joseph – Institut de Chimie de Strasbourg, UMR 7177 CNRS-Université de Strasbourg, 4 rue Blaise Pascal, 67008 Strasbourg, France
Jean Weiss – Institut de Chimie de Strasbourg, UMR 7177 CNRS-Université de Strasbourg, 4 rue Blaise Pascal, 67008 Strasbourg, France
Can Wang – ISIS, UMR 7006 CNRS-Université de Strasbourg, 8 allée Gaspard Monge, BP 70028, 67083 Strasbourg, France
Artur Cieselski - ISIS, UMR 7006 CNRS-Université de Strasbourg, 8 allée Gaspard Monge, BP 70028, 67083 Strasbourg, France

Present Addresses

§ **Jimmy Richard** - Institut des Sciences Moléculaires Université de Bordeaux - CNRS UMR 5255 Bâtiment A12, 351 cours de la libération 33405 TALENCE cedex, France.

Author Contributions

All authors have given approval to the final version of the manuscript. & These authors contributed equally.

ACKNOWLEDGMENT

The authors acknowledge funding from the Agence Nationale de la Recherche through the Labex project CSC (ANR-10-LABX-0026 CSC) within the Investissement d'Avenir program (ANR-10-120 IDEX-0002- 02), the International Center for Frontier Research in Chemistry (icFRC, JWE-CSC-0003) and the ERC project SUPRA2DMAT (GA-833707). We thank the Institut de Chimie de Strasbourg (UMR 7177, CNRS-Université de Strasbourg) for a Master's 2 fellowship for JJ.

REFERENCES

(1) For a recent and thorough review see: Constable, E. C.; Housecroft, C. E. The Early Years of 2,2'-Bipyridine: A Ligand in its Own Lifetime. *Molecules* **2019**, *24*, 3951.

(2) Biradha, K.; Sarkar, M.; Rajput, L. Crystal Engineering of Coordination Polymers Using 4,4'-Bipyridine as a Bond Between Transition Metal Atoms. *Chem. Commun.* **2006**, 4169–4179.

(3) (a) Feng, X.; Feng, Y.; Guo, N.; Sun, Y.; Zhang, T.; Ma, L.; Wang, L. Series d-f Heteronuclear Metal-Organic Frameworks: Color Tunability and Luminescent Probe with Switchable Properties. *Inorg. Chem.* **2017**, *56*, 1713–1721. (b) Chen, Z.; Zhang, S.; Zhang, S.; Sun, Q.; Xiao, Y.; Wang, K. Cadmium-Based Coordination Polymers from 1D to 3D: Synthesis, Structures, and Photoluminescent and Electrochemiluminescent Properties. *ChemPlusChem* **2019**, *84*, 190–202.

(4) (a) Yan, F.-F.; Zhang, R.-F.; Ru, J.; Ma, C.-L. Self-Assembly and Characterization of a 2D Polymer Containing Hexanuclear 78-Membered Organotin Macrocycles and a 1D Right-Handed Helical Organotin Chain. *J. Organomet. Chem.* **2018**, *866*, 43–49. (b) Bhowmick, S.; Chakraborty, S.; Das, A.; Nallapeta, S.; Das, N. Pyrazine Motif Containing Hexagonal Macrocycles: Synthesis, Characterization, and Host-Guest Chemistry with Nitro Aromatics. *Inorg. Chem.* **2015**, *54*, 8994–9001.

(5) (a) Fujita, M.; Yazaki, J.; Ogura, K. Preparation of a Macrocyclic Polynuclear Complex, $[(en)Pd(4,4'\text{-bpy})]_4(NO_3)_8$ (en = Ethylenediamine, bpy = Bipyridine), which Recognizes an Organic Molecule in Aqueous Media. *J. Am. Chem. Soc.* **1990**, *112*, 5645–5647. (b) Kuehl, C. J.; Huang, S. D.; Stang, P. J. Self-Assembly with Postmodification: Kinetically Stabilized Metalla-Supramolecular Rectangles. *J. Am. Chem. Soc.* **2001,** *123*, 9634–9641. (c) Liao, R. T.; Yang, W. C.; Thanasekaran, P.; Tsai, C. C.; Sathiyendiran, M.; Liu, Y. H.; Rajendran, T.; Lin, H. M.; Tseng, T. W.; Lu, K. L. Rhenium-Based Molecular Rectangular Boxes with Large Inner Cavity and High Shape Selectivity Towards Benzene Molecule. *Chem Commun*. **2008**, 3175–3177. (d) Fujita, M.; Oguro, D.; Miyazawa, M.; Oka, H.; Yamaguchi, K.; Ogura, K. Self-Assembly of Ten Molecules into a Nanometer-Sized Organic Host Frameworks. *Nature* **1995**, *378*, 469–471. (e) Stang, P. J.; Cao, D. H.; Saito, S.; Arif, A. M. Self-Assembly of Cationic, Tetranuclear, Pt(II) and Pd(II) Macrocyclic Squares. X-ray Crystal Structure of $[Pt^{2+}(dppp)(4,4'\text{-bipyridyl})_2\text{-}OSO_2CF_3]_4$. *J. Am. Chem. Soc.* **1995**, *117*, 6273–6283.

(6) (a) Zhang, Z.-X.; Ding, N.-N.; Zhang, W.-H.; Chen, J.-X.; Young, D. J.; Hor, T. S. A. Stitching 2D Polymeric Layers into Flexible Interpenetrated Metal-Organic-Frameworks within Single Crystals. *Angew. Chem. Int. Ed. Engl.* **2014**, 53, 4628–4632. (b) Zhou, M.; Yan, D.; Dong, Y.; He, X.; Xu, Y. Chiral $[Mo_8O_{26}]^{4-}$ Polyooxoanion-Induced Three-Dimensional Architectures with Homochiral Eight-Fold Interpentrated Metal-Organic-Frameworks. *Inorg. Chem.* **2017**, *56*, 9036–9043.

(7) (a) Li, J.; Chen, S.; Jiang, L.; Wu, D.; Li, Y. Pore Space Partitioning of Metal-Organic Framework for C2Hx Separation from Methane. *Inorg. Chem*. **2019**, *58*, 5410–5413. (b) Cheng, J.; Liang, J.; Dong, L.; Chai, J.; Zhao, N.; Ullah, S.; Wang, H.; Zhang, D.; Imtiaz, S.; Shan, G.; Zheng, G. Self-assembly of 2D-Metal-Organic Framework/Graphene Oxide Membranes as Highly Efficient Adsorbents for the Removal of Cs^+ from Aqueous Solutions. *RSC Adv*. **2018**, *8*, 40813–40822.

(8) (a) Li, S.; Lu, L.; Zhu, M.; Feng, S.; Su, F.; Zhao, X. Exploring the Syntheses, Structures, Topologies, Luminescence Sensing and Magnetism of Zn(II) and Mn(II) Coordination Polymers Based on a Semi-Rigid Tricarboxylate Ligand. *CrystEngComm.* **2018**, *20*, 5442–5456. (b) Zhang, Y.; Wang, J. Ancillary Ligand-Controlled Assembly of Three

Coordination Polymers: Synthesis, Characterization, Luminescent, and Catalytic Properties. *J. Coord. Chem*. **2018**, *71*, 2632–2645.

(9) (a) Zhao, W.; Wang, W.; Peng, J.; Chen, T.; Jin, B.; Liu, S.; Huang, W.; Zhao, Q. Wrinkled Two-Dimensional Ultrathin Cu(II)-Porphyrin Framework Nanosheets Hybridized with Polypyrrole for Flexible All-Solid-State Supercapacitors. *Dalton Trans.* **2019,** *48*, 9631–9638. (b) Cheng, J.; Chen, S.; Chen, D.; Dong, L.; Wang, J.; Zhang, T.; Jiao, T.; Liu, B.; Wang, H.; Kai, J.-J.; Zhang, D.; Zheng, G.; Zhi, L.; Kang, F.; Zhang, W. Editable Asymmetric All-Solid-State Supercapacitors Based on High-Strength, Flexible, and Programmable 2D-Metal-Organic Framework/Graphene Oxide Self-Assembled Papers. *J. Mat. Chem. A* **2018**, *6*, 20254–20266.

(10) Chen, T.; Pan, G.-B.; Wettach, H.; Fritzsche, M.; Höger, S.; Wan, L.-J.; Yang, H.-B.; Northrop, B. H.; Stang, P. J. 2D Assembly of Metallacycles on HOPG by Shape-Persistent Macrocycle Templates *J. Am. Chem. Soc.* **2010**, *132*, 1328–1333.

(11) (a) Li, M.; Yang, Y.-L.; Zhao, K.-Q.; Zeng, Q.-D.; Wang, C. Bipyridine-Mediated Assembling Characteristics of Aromatic Acid Derivatives. *J. Phys. Chem. C* **2008**, *112*, 10141–10144. (b) Xu, B.; Yin, S.; Wang, C.; Zeng, Q.; Qiu, X.; Bai, C. Identification of Hydrogen Bond Characterizations of Isomeric 4Bpy and 2Bpy by STM. *Surf. Interface Anal.* **2001**, *32*, 245–247.

(12) (a) Qian, Y.; Gu, Y.; Feng, J.; Jiang, W.; Geng, Y.; Duan, W.; Ma, J.; Zeng, Q.; Wang, Z. Role of Synergistic C – H ··· N and C – H ··· O H - Bonding Interactions in Self-Assemblies of a Phthalocyanine Derivative and Several Pyridine Derivatives. *J. Phys. Chem. C* **2018**, *122*, 24158–24163. (b) Xu, S.; Yin, S.; Xu, S. Tunable Linear Nanopatterns of Disubstituted Alkane Derivatives Containing Bi-Components via Selective Hydrogen Bonding. *Appl. Phys. A* **2010**, *99*, 99–103.

(13) (a) Langner, A.; Tait, S. L.; Lin, N.; Chandrasekar, R.; Meded, V.; Fink, K.; Ruben, M.; Kern, K. Selective Coordination Bonding in Metallo-supramolecular Systems on Surfaces. *Angew. Chem. Int. Ed.* **2012**, *51*, 4327–4331. (b) Tait, S. L.; Langner A.; Lin, N.; Stepanow, S.; Rajadurai, C.; Ruben, M.; Kern, K. One-dimensional Self-Assembled Molecular Chains on Cu(100): Interplay between Surface-Assisted Coordination Chemistry and Substrate Commensurability. *J. Phys. Chem. C* **2007**, *111*, 10982–10987.

(14) Pang, J. H.; Kaga, A.; Roediger, S.; Lin, M. H.; Chiba, S. Revisiting the Chichibabin Reaction: C2 Amination of Pyridines with a NaH-Iodide Composite. *Asian J. Org. Chem.* **2019**, *8*, 1058–1060.

(15) (a) Kelly, T. R.; Lee, Y.-J.; Mears, R. J. Synthesis of Cyclo-2,2':4',4'':2'',2''':4''',4'''':2'''',2''''':4''''',4-sexipyridine. *J. Org. Chem*. **1997**, *62*, 2774–2781. (b) Mastalir, M.; Pittenauer, E.; Allmaier, G.; Kirchner, K. 2,6-Diamination of Substituted Pyridines via Heterogeneous Chichibabin Reaction. *Tetrahedron Lett.* **2016**, *57*, 333–336.

(16) (a) Citterio, A.; Arnoldi, A.; Macri, C. Nucleophilic Character of Acyl Radicals. Homolytic Acetylation of 4,4'-Bipyridine. *Chim. Ind*. **1978**, *60*, 14–15. (b) Barbaro, P.; Bianchini, C.; Giambastiani, G.; Guerrero Rios, I.; Meli, A.; Oberhauser, W.; Segarra, A. M.; Sorace, L.; Toti, A. Synthesis of New Polydentate Nitrogen Ligands and Their Use in Ethylene Polymerization in Conjunction with Iron(II) and Cobalt(II)Bis-halides and Methylaluminoxane. *Organometallics*, **2007**, *26*, 4639–4651.

(17) Lieb, D.; Friedel, F. C.; Yawer, M.; Zahl, A.; Khusniyarov, M. M.; Heinemann, F. W.; Ivanović-Burmazović, I. Dinuclear Seven-Coordinate Mn(II) Complexes: Effect of Manganese(II)-Hydroxo Species on Water Exchange and Superoxide Dismutase Activity. *Inorg. Chem.* **2013**, *52*, 222–236.

(18) Barltrop, J. A.; Jackson, A. C. The Synthesis and Electrochemical Study of New Electrochromic Viologen-Based Materials. *J. Chem. Soc. Perkin Trans. 2*, **1984**, 367–371.

(19) Zassowski, P.; Golba, S.; Skorkac, L.; Szafraniec-Gorol, G.; Matussek, M.; Zych, D.; Danikiewicz, W.; Krompiec, S. Lapkowski, M.; Slodek, A.; Domagala, W. Spectroelectrochemistry of Alternating Ambipolar Copolymers of 4,4'- and 2,2'-Bipyridine Isomers and Quaterthiophene. *Electrochim. Acta*, **2017**, *231*, 437–452.

(20) Yin, G.-J.; Ji, B.-M.; Du, C.-X. In Situ Hydrothermal Synthesis of Two Novel Cd(II) Coordination Compounds. *Inorg. Chem. Commun.* **2012**, *15*, 21–24.

(21) Gatenyo, J.; Hagooly, Y.; Vints, I.; Rozen, S. Activation of a CH Bond in Polypyridine Systems by Acetyl Hypofluorite Made from F_2. *Org. Biomol. Chem*. **2012**, *10*, 1856–1860.

(22) (a) Schmalzl, K.; Summers, L. Chemical Constitution and Activity of Bipyridylium Herbicides. XII. Diquaternary Salts of 6-Methyl-2,2'-bipyridyl and 2-Methyl-4,4'-bipyridyl. *Aust. J. Chem*. **1977**, *30*, 657–662. (b) Rank, M.; Zabel, M.; Winter, R. F. Pyridine vs. Bipyridine Coordination in $PtCl_2$ Complexes of 4-*t*Butyl-4'-(4-pyridinyl)-2,2'-bipyridine. *Z. Anorg. Allg. Chemie* **2013**, *639*, 2565–2574.

(23) Rebek, J.; Costello, T.; Wattley, R. Binding Forces and Catalysis. The Use of Bipyridyl-Metal Chelation to Enhance Reaction Rates. *J. Am. Chem. Soc.* **1985**, *107*, 7487–7493.

(24) Awad, H.; Mongin, F.; Trécourt, F.; Quéguiner, G.; Marsais, F. Deprotonation of Chloropyridines using Lithium Magnesates. *Tetrahedron Lett*. **2004**, *45*, 7873–7877.

(25) Abboud, M.; Mamane, V.; Aubert, E.; Lecomte, C.; Fort, Y. Synthesis of Polyhalogenated 4,4'-Bipyridines via a Simple Dimerization Procedure. *J. Org. Chem.* **2010**, *75*, 3224–3231.

(26) Iyoda, M.; Otsuka, H.; Sato, K.; Nisato, N.; Oda, M. Homocoupling of Aryl Halides Using Nickel(II) Complex and Zinc in the Presence of Tetraethylammonium Iodide. An Efficient Method for the Synthesis of Biaryls and Bipyridines. *Bull. Chem. Soc. Jpn*. **1990**, *63*, 80–87.

(27) Kallweit, C.; Haberhauer, G.; Woitschetzki, S. 4,4'-Bipyridine as a Unidirectional Switching Unit for a Molecular Pushing Motor. *Chem. Eur. J.* **2014**, *20*, 6358–6365.

(28) Durben, S.; Baumgartner, T. 3,7-Diazadibenzophosphole oxide: A Phosphorus-Bridged Viologen Analogue with Significantly Lowered Reduction Threshold. *Angew. Chem. Int. Ed.* **2011**, *50*, 7948–7952.

(29) Cahiez, G.; Chaboche, C.; Mahuteau-Betzer, F.; Ahr, M. Iron-catalyzed homo-coupling of simple and functionalized arylmagnesium reagents. *Org. Lett*. **2005**, *7*, 1943–1946.

(30) (a) Swahn, B.-M.; Xue, Y.; Arzel, E.; Kallin, E.; Magnus, A.; Plobeck, N.; Viklund, J. Design and Synthesis of 2′-Anilino-4,4′-bipyridines as Selective Inhibitors of c-Jun N-Terminal Kinase-3. *Bioorg. Med. Chem. Lett*. **2006**, *16*, 1397–1401. (b) Benniston, A. C.; Harriman, A.; Li, P.; Rostron, J. P.; Harrington, R. W.; Clegg, W. A Spectroscopic Study of the Reduction of Geometrically Restrained Viologens. *Chem. Eur. J.* **2007**, *13*, 7838–7851.

(31) Hilton, M. C.; Zhang, X.; Boyle, B. T.; Alegre-Requena, J. V.; Paton, R. S.; McNally, A. Heterobiaryl Synthesis by Contractive C–C coupling via P(V)Intermediates. *Science* **2018**, *362*, 799–804.

(32) Baumann, K. L.; Byker, H. J.; Guarr, T. F.; Siegrist, K. E.; Theiste, D. A.; Winkle, D. D. An Improved Electrochromic Medium Capable of Producing a Pre-Selected Color. PCT Int. Appl., 9844384, 08 Oct 1998.

(33) A. Fürstner, A.; Leitner, A.; Méndez, M.; Krause, H. Iron-Catalyzed Cross-Coupling Reactions. *J. Am. Chem. Soc.* **2002**, *124*, 13856–13863.

(34) Lüning, U.; Baumstark, R.; Müller, M. Concave Pyridines and 1,10-Phenanthrolines with Sulfonamide Bridgeheads. Increased Basicity by 4-Diethylamino Substitution of the Pyridine Unit. *Liebigs Ann. Chem.* **1991**, 987–988.

(35) Dietrich, J.; Josef, K. Invertseifen als Anti-mykotika; Zusammenhänge zwischen Konstitution und Wirkung. *Chem. Ber.* **1950**, *83*, 277–287.

(36) Browne, C.; Brenet, S.; Clegg, J. K.; Nitschke, J. R. Solvent-Dependent Host–Guest Chemistry of an Fe_8L_{12} Cubic Capsule. *Angew. Chem. Int. Ed.* **2013**, *52*, 1944–1948.

(37) Leighton, P.; Sanders, J. K. M. Synthesis of Bipyridyl-, Viologen-, and Quinone-bridged Porphyrins. *J. Chem. Soc., Perkin Trans. 1* **1987**, 2385-2393.

(38) Boekelheide, V.; Linn, W. J. Rearrangements of *N*-Oxides. A Novel Synthesis of Pyridyl Carbinols and Aldehydes *J. Am. Chem. Soc.* **1954**, *76*, 1286–1291.

(39) Aoyama, T.; Sonoda, N.; Yamauchi, M.; Toriyama, K.; Anzai, M.; Ando, A.; Shioiri, T. Chemical Manganese Dioxide (CMD), an Efficient Activated Manganese Dioxide. Application to Oxidation of Benzylic and Allylic Alcohols. *Synlett* **1998**, 35–36.

(40) Yang, M.; Mao, D.; Chen, S.; Zhang, H. Design, Synthesis and Thermotropic Self-Organization of Dendronized Polystyrenes with Different Length Alkyl Tails. *Polym. Chem.* **2016**, *7*, 5445–5455.

(41) Dougherty, T. K.; Lau, K. S. Y.; Hedberg, F. L. Anomaly in Palladium-Catalyzed Phenylethynylation of 2,2'-Dihalobiphenyls: Formation of Alkylidenefluorenes. *J. Org. Chem.* **1983**, *48*, 5273–5280.

(42) Boag, N. M.; Coward, K. M.; Jones, A. C.; Pemble, M. E.; Thompson, J. R. 4,4'-bipyridyl at 203 K. *Acta Cryst. C* **1999**, 55, 672 –674.

(43) Gourdon, A. 3,3'-Dimethyl-4,4'-bipyridine and 5,5'-dimethyl-4,4'-bipyrimidine. *Acta Cryst. C* **1993**, *49*, 1011 – 1013.

(44) Kikkawa, Y. 2D Structural Modulation by Odd-Even Effect of Alkyl Chains Revealed by Scanning Tunneling Microscopy at Solid/liquid Interface. *Trans. Mat. Res. Soc. Japan* **2014**, *39*, 99 –104.

(45) Scherer, L. J.; Merz, L.; Constable, E. C.; Housecroft, C. E.; Neuburger, M.; Hermann, B. A. Conformational Analysis of Self-Organized Monolayers with Scanning Tunneling Microscopy at Near-Atomic Resolution. *J. Am. Chem. Soc.* **2005**, *127*, 4033 –4041.

(46) Ivchenko, P. V.; Nifant'eva, I. E.; Buslov, I. V. A Convenient Approach for the Synthesis of 2,6-Diformyl- and 2,6-Diacetylpyridines. *Tetrahedron Lett.* **2013**, *54*, 217–219.

(47) Martinez-Palau, M.; Perea, E.; Lopez-Calahorra, F.; Velasco, D. Synthesis of luminescent *N*-arylcarbazoles by copper bronze-mediated reaction. *Lett. Org. Chem.* **2004**, *1*, 231–237.

Entry for the Table of Contents

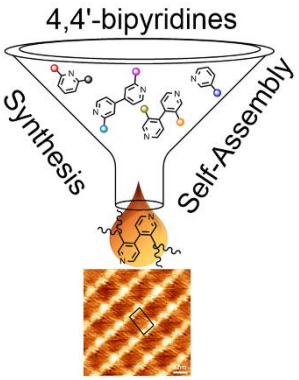

4,4'-Bipyridines line up for applications as new versatile synthetic methods enrich their functionalization at 2,2',6,6' and 3,3' positions. When alkyl chains are selectively introduced, these compounds self-assemble into 2D nanopatterns on HOPG, as demonstrated by STM studies.